Chalcogenide Letters Vol. 19, No. 12, December 2022, p. 891 - 899

# Synthesis, structure and properties of $PbO–PbF_2–B_2O_3–SiO_2$ glasses

Yu. S. Hordieiev*, A. V. Zaichuk
*Ukrainian State University of Chemical Technology, 8 Gagarin Avenue, Dnipro, 49005, Ukraine*

The structure, thermal and some physical properties of lead fluoroborate glasses containing 30 mol% $SiO_2$ have been investigated by differential thermal analysis, X-ray diffraction and Fourier-transform infrared spectroscopy. The glasses were prepared by the conventional melt-quenching method. Fourier-transform infrared spectroscopy results showed that the network of these glasses consists mainly of $BO_3$, $BO_4$, $SiO_4$, and $PbO_4$ structural units. The thermal stability of the glass samples determined by differential thermal analysis was found to be about 80°C. Dilatometric measurements showed that the glass transition temperature and dilatometric softening temperature decrease with increasing lead content, whereas the coefficient of thermal expansion increases. The density and molar volume increased with the increase in lead content. The conductivity of the investigated glasses mainly depends on the mobility of $F^-$ and $Pb^{2+}$ ions. The variation in volume resistance upon changing the composition has been correlated with the structural changes in the glass network. The results obtained in this study indicate that the investigated glasses can be potential candidates for advanced technologies as solder and sealing materials.

(Received September 2, 2022; Accepted December 6, 2022)

*Keywords:* Fluoroborate glasses, Glass transition, Thermal expansion, Volume resistance, Glass structure

## 1. Introduction

Lead fluoroborate glasses and glass-ceramics have recently attracted growing attention in both scientifically and technologically due to their unique properties and promising potential applications in photonics, optoelectronic and electrochemical applications [1–6]. These glasses have some interesting features, such as low melting points, wide glass-formation region [3], high chemical durability, high refractive index [4], and good radiation shielding for γ-rays [5], and are regarded as a basis for manufacturing various coatings, solder glasses, glass-to-metal seals, optical lenses, and as a potential material for radioactive waste immobilization [7–12]. However, for most of these materials, the relationship between composition-structure-property is not well understood, making improving their properties difficult. Therefore, numerous studies are still being carried out on this topic.

Lead fluoroborate glasses can be synthesized in a wide range of compositions with $PbF_2$ content from 20 to 60 mol % and PbO from 5 to 70 mol % [2, 3]. Lead oxide is used as a component of silicate, phosphate, and borate glasses to achieve useful physical properties, and although it is not itself a glass-forming oxide, it can be included in significant amounts in these glass-forming systems [13, 14]. It is well known that the introduction of lead oxide into a borate matrix leads to the creation of trigonal [$BO_3$] and tetrahedral [$BO_4$] structural units [13–15]. The equilibrium of the structural conversion between [$BO_3$] and [$BO_4$] units in the borate network depends on the chemical composition and the kind of modifiers [15]. The addition of lead fluoride to borate glasses decreases the phonon energy, increases the moisture resistance and transparency in the visible region, and plays an important role in forming a three-dimensional network structure [16].

* Corresponding author: yuriihordieiev@gmail.com
https://doi.org/10.15251/CL.2022.1912.891

Although the lead fluoroborate glasses exhibit excellent physical properties, they also exhibit poor thermal stability against devitrification, which is common to most oxyfluoride glasses [3, 17]. Improvements in the thermal stability of glass against devitrification can often be achieved by increasing the number of components [2, 17–19]. The addition of some oxides, especially $SiO_2$, to oxyfluoride glass melts increases the glass stability against crystallization and helps stabilize the glass state. The results of some studies show that oxyfluoride glasses containing 20–30 mol% $SiO_2$ have excellent thermal stability of glass against devitrification while maintaining key properties, such as low melting points and high chemical durability [2, 20–22].

Therefore, the aim of this study was to prepare lead fluoroborate glasses containing 30 mol% $SiO_2$ and to investigate their structure, thermal behavior, and physical properties to obtain new materials with prospective applications.

## 2. Materials and methods

The details of the batch composition of the investigated glasses with their label are given in Table 1. Reagent-grade chemicals of $Pb_3O_4$, $H_3BO_3$, $SiO_2$, and $PbF_2$ were used as starting raw materials. The glass batches were prepared by mixing an appropriate mole fraction of the desired oxide ingredients in an agate mortar with a pestle to ensure complete homogeneity. The homogeneous glass batches were melted in the alumina crucibles with the volume of 50 mL in an electric furnace with silicon carbide heaters at the temperature of 950ºC for 30 min in an air atmosphere. The homogeneous melts were quickly cast onto a preheated stainless-steel mold to obtain glasses which were then transferred into a muffle furnace preset to 300°C.

*Table 1. Chemical composition (mol %) of the investigated glasses.*

| Glass sample No. | PbO | $PbF_2$ | $B_2O_3$ | $SiO_2$ |
|---|---|---|---|---|
| 1 | 7 | 21 | 42 | 30 |
| 2 | 7 | 28 | 35 | 30 |
| 3 | 7 | 35 | 28 | 30 |
| 4 | 7 | 42 | 21 | 30 |
| 5 | 7 | 49 | 14 | 30 |
| 6 | 14 | 21 | 35 | 30 |
| 7 | 14 | 28 | 28 | 30 |
| 8 | 14 | 35 | 21 | 30 |
| 9 | 14 | 42 | 14 | 30 |
| 10 | 21 | 21 | 28 | 30 |
| 11 | 21 | 28 | 21 | 30 |
| 12 | 21 | 35 | 14 | 30 |
| 13 | 28 | 21 | 21 | 30 |
| 14 | 28 | 28 | 14 | 30 |
| 15 | 35 | 21 | 14 | 30 |

The crystallization ability of glass powders was determined by differential thermal analysis on the derivatograph Q-1500D at a heating rate of 5°C/min from room temperature to 800°C in an air atmosphere. Alumina oxide fired at the temperature of 1450°C was used as a reference.

Crystalline phases precipitated during heat treatment were identified by X-ray diffractometer DRON-3M using Co-$K_\alpha$ radiation in the $10 < 2\Theta < 90$ range.

The FTIR spectra of the glasses were recorded in the 1550–400 $cm^{-1}$ region using the KBr pellet technique (Thermo Nicolet Avatar 370 FTIR Spectrometer).

The thermal expansion coefficient (TEC), glass transition temperature ($T_g$), and dilatometric softening point ($T_d$) of the glass samples were determined using a dilatometer (Dilatometer1300 L, Italy) at a heating rate of 3°C/min. The TEC value was calculated between 20 and 200°C, and repeated measurements indicated the thermal expansion coefficient with an error of ±2 ppm/ºC. The density of the glasses was determined by the Archimedes principle using toluene as the immersion liquid and a digital balance of sensitivity of $10^{-3}$ g. The weight of each glass sample was measured three times, and an average was taken to minimize the sources of error. The volume resistivity of the investigated glasses was measured on flat-parallel plates in a cell with graphite electrodes in the temperature range of 50–250°C at a heating rate of 5°C/min using the teraohmmeter E6–13A.

## 3. Results and discussion

All obtained glass samples after melting at 950°C for 30 min were transparent and bubble-free (Fig. 1). The colour of the samples gradually changed to darker shades of yellow with the substitution of $B_2O_3$ by PbO. The amorphous nature of the obtained glass samples was checked by X-ray diffraction, which shows (Fig. 2) a broad halo pattern typical for a fully amorphous structure.

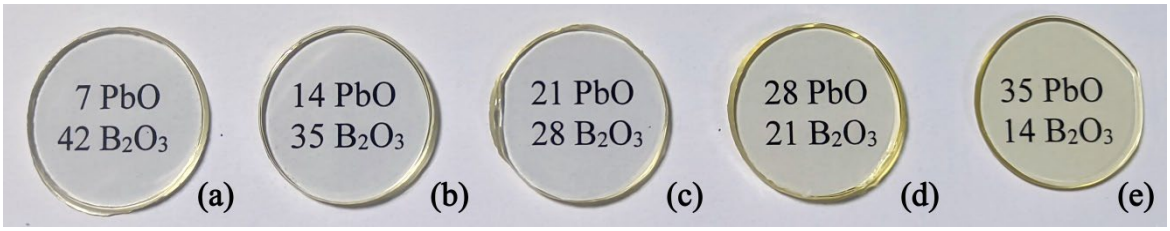


*Fig. 1. Samples of some obtained glasses: (a) No. 1, (b) No. 6, (c) No. 10, (d) No. 13 and (e) No. 15.*

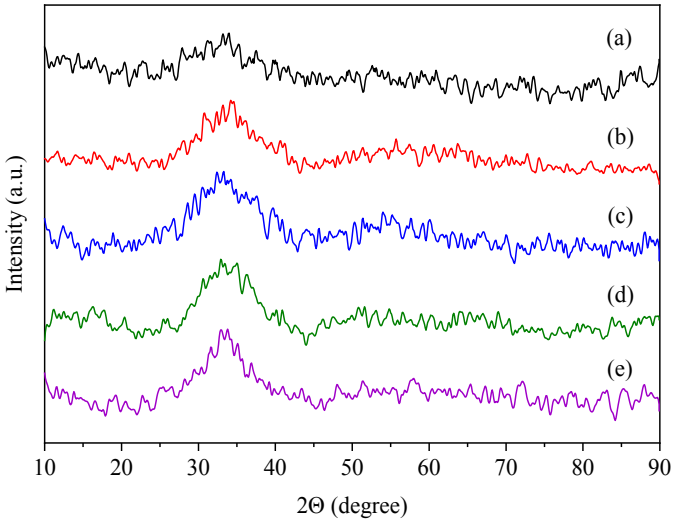


*Fig. 2. X-ray diffraction patterns of glass samples: (a) No. 1, (b) No. 6, (c) No. 10, (d) No. 13 and (e) No. 15.*

Differential thermal analysis (DTA) was employed to determine the thermal behavior of the investigated glasses. DTA thermograms of $PbO–PbF_2–B_2O_3–SiO_2$ glasses in the temperature range of 200–700°C are shown in Fig. 3 according to the equimolar substitution of $B_2O_3$ by PbO at constant $SiO_2$ and $PbF_2$. The onset of the endothermic and exothermic peaks is commonly used to

determine the glass transition temperature and onset crystallization temperatures, and the peak crystallization temperature is defined as the maximum at the exothermic peak [23, 24]. All glass samples showed the onset of slope change of the DTA curves between 350 and 410°C, corresponding to the glass transition. The glass transition temperature gradually decreased with increasing PbO content. In addition to the glass transition temperature, all the samples exhibit a very weak exothermic peak between 430 and 510°C. The observed decrease in glass transition and crystallization temperatures with the equimolar substitution of $B_2O_3$ by PbO is probably associated with the substitution of stronger B–O bonds by weaker Pb–O bonds, which leads to an increase in the looseness of packing within the structure [25]. The temperature difference between the onset of crystallization and glass transition ($\Delta T = T_c - T_g$) gives a gauge of the glass's resistance to crystallizing upon heating [26]. $\Delta T$ values for investigated glass samples were greater than 80°C and slightly increased, from 80 to 100°C with increasing $B_2O_3$ content.

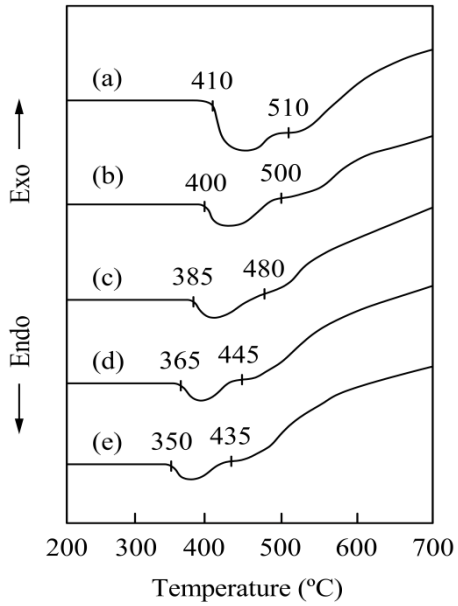


*Fig. 3. DTA curves of the glass powder samples: (a) No. 1, (b) No. 6, (c) No. 10, (d) No. 13 and (e) No. 15.*

In order to identify the crystalline phase corresponding to the exothermic peak in the DTA curves, the glass powder was heat-treated at around the crystallization temperature in the air for 1 and 10 hours. X-ray diffraction phase analysis (Fig. 4) showed no significant changes in glass sample No.1 after 1 h of heat treatment. However, the crystalline phase of PbO (ICSD 015403) is formed after 10 h of heat treatment.

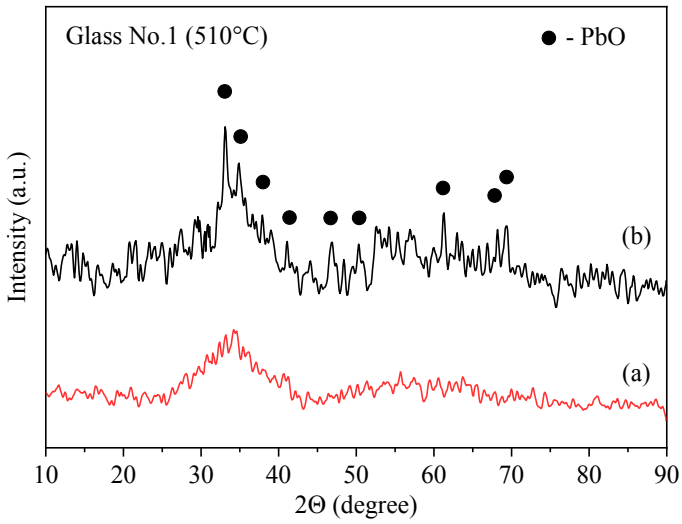


*Fig. 4. X-ray diffraction pattern of glass powder heat-treated at the crystallization temperature in the air for 1 (a) and 10 (b) hours.*

Fourier-transform infrared spectroscopy (FTIR) is a powerful tool for understanding how the local structure of glass changes due to its composition. FTIR spectra (Fig. 5) of PbO–$PbF_2$–$B_2O_3$–$SiO_2$ glasses were analyzed in order to obtain information on the structural transformations in the glass network following the equimolar substitution of $B_2O_3$ by PbO at constant $SiO_2$ and $PbF_2$. The FTIR spectra of the investigated glasses include two main broad bands at 800–1200 $cm^{-1}$ and 1200–1500 $cm^{-1}$. In addition, there are two small bands below 800 $cm^{-1}$. The lead and borate groups have been observed to play a dominant role in the spectra of the investigated glasses. The broad band observed at 1200–1500 $cm^{-1}$ centered at ~1360 $cm^{-1}$ is attributed to stretching vibrations of [$BO_3$] units with non-bridging oxygens (NBOs) [27–31]. Its relative area decreases with an increase in PbO content with shifting of its center towards slightly lower wavenumbers. The band in the range 800–1200 $cm^{-1}$ overlaps with the stretching vibration of [$SiO_4$] structural units and contains the stretching vibration of [$BO_4$] structural units [32, 33]. The relative area of this band increases with an increase in the PbO content from 7 to 28 mol%, with a shift of its center towards slightly lower wavenumbers. This indicates that the addition of PbO leads to the conversion of [$BO_3$] units to [$BO_4$] units in the investigated glass. With further increase in the PbO content (>28 mol %), the rate of formation of [$BO_4$] units is reduced because some of the PbO is used up in the formation of [$PbO_4$] structural units. As the PbO content increase, the bending vibration frequency of B–O–B in [$BO_3$] units shifts from 680 $cm^{-1}$ to a higher wavenumber 700 $cm^{-1}$ [27–30]. The absorption band centered at 620 $cm^{-1}$ can be assigned to the bending vibration of B–O–Pb linkages in the bridge connection of [$BO_3$] and [$BO_4$] units [29]. In light of the above discussions, it can be concluded that, with an increase in the PbO content, B–O–B bonds, which are the dominant structural linkages at low PbO content, give way to B–O–Pb bonds and, ultimately, to Pb–O–Pb linkages (~560 $cm^{-1}$) at higher PbO content. The absorption band at about 470 $cm^{-1}$ is assumed to be due to the combined vibration of [$SiO_4$] and [$PbO_4$] groups [34–36].

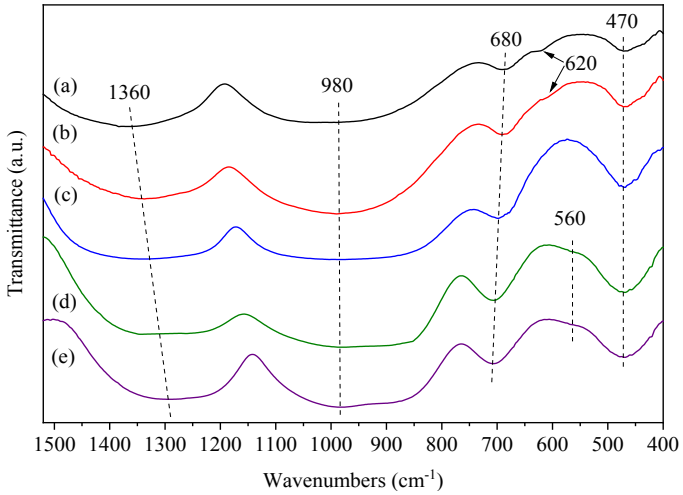


*Fig. 5. FTIR spectra of glass samples: (a) No. 1, (b) No. 6, (c) No. 10, (d) No. 13 and (e) No. 15.*

It is well known that the physical properties of glasses are closely related to their structure and composition. The physical properties of the investigated glasses were investigated by measuring the volume resistivity, thermal expansion coefficient, glass transition temperature, dilatometric softening point, density, and calculating the molar volume values. The obtained values are given in Table 2. The obtained results showed that the density (4.48–5.68 g/cm$^3$) and molar volume (25.53–29.15 cm$^3$/mol) values of the investigated glasses were increased with increasing lead content. The increase in the density is due to the relatively larger molar mass of lead oxide than other glass components, while the large ionic radius of the lead ions causes an increase in the molar volume. It can be seen from the dilatometry results that the dilatometric softening point (340–420ºC) and glass transition temperature (320–390ºC) of the investigated glasses were decreased with equimolar substitution of $B_2O_3$ by PbO or $PbF_2$ at a constant $SiO_2$ content. These glasses also showed increased TEC values from 7.1 to 10.9 ppm/ºC, with increasing lead content. The weaker glass network connectivity and higher polarisability of non-bridging oxygens formed with the substitution of stronger B–O bonds by weaker Pb–O bonds explain the increase in TEC values and the shift of $T_g$ and $T_d$ towards lower temperature [37].

*Table 2. The values of the glass transition temperature ($T_g$), dilatometric softening point ($T_d$), thermal expansion coefficient (TEC), density (d), molar volume ($V_m$), volume resistivity (lgρ) of the investigated glasses.*

| Glass sample No. | $T_g$, (ºC) | $T_d$, (ºC) | TEC, (ppm/ºC) | d, (g/cm$^3$) | $V_m$, (cm$^3$/mol) | lgρ at 200°C (Ohm·cm) |
|---|---|---|---|---|---|---|
| 1 | 390 | 420 | 7.1 | 4.48 | 25.53 | $6.3\cdot10^{11}$ |
| 2 | 375 | 400 | 8.3 | 4.89 | 25.90 | $2.1\cdot10^{9}$ |
| 3 | 355 | 385 | 8.9 | 5.24 | 26.52 | $0.5\cdot10^{8}$ |
| 4 | 330 | 360 | 9.9 | 5.51 | 27.45 | $4.7\cdot10^{7}$ |
| 5 | 320 | 350 | 10.2 | 5.61 | 29.15 | $8.1\cdot10^{6}$ |
| 6 | 370 | 400 | 8.2 | 4.85 | 25.80 | $4.4\cdot10^{10}$ |
| 7 | 355 | 385 | 8.7 | 5.21 | 26.38 | $5.5\cdot10^{8}$ |
| 8 | 340 | 360 | 9.6 | 5.43 | 27.57 | $6.3\cdot10^{7}$ |
| 9 | 335 | 355 | 9.8 | 5.59 | 28.98 | $1.2\cdot10^{7}$ |
| 10 | 360 | 380 | 8.9 | 5.19 | 26.18 | $3.5\cdot10^{9}$ |
| 11 | 340 | 360 | 10 | 5.35 | 27.70 | $0.75\cdot10^{8}$ |
| 12 | 320 | 350 | 10.7 | 5.55 | 28.91 | $3.2\cdot10^{7}$ |
| 13 | 345 | 370 | 9.5 | 5.37 | 27.31 | $3.9\cdot10^{8}$ |
| 14 | 320 | 340 | 10.9 | 5.67 | 28.03 | $6.7\cdot10^{7}$ |
| 15 | 320 | 345 | 10.5 | 5.68 | 27.71 | $2.7\cdot10^{8}$ |

At the temperature of 200ºC, the volume resistivity of the investigated glasses is in the range of $10^6$–$10^{11}$ Ohm·cm. The volume resistivity decreases with increasing $PbF_2$ content in the investigated glass. Since $F^-$ ions can be considered the dominant charge carriers in these glasses, such a change in volume resistivity is expected [13]. An increase in the PbO content loosens the glass network, facilitating the migration of conducting ions, such as $F^-$ ions and possibly $Pb^{2+}$ ions [3], which also contribute to conduction processes in such glasses. In the case of $B_2O_3$, the equimolar substitution of PbO by $B_2O_3$ leads to a significant increase in volume resistivity due to the more compact arrangement of borate structural groups, resulting in a reduction in the space in which conductive ions can move.

## 4. Conclusions

The structure, thermal and some physical properties of lead fluoroborate glasses containing 30 mol% $SiO_2$ were investigated. The main building units forming the glass network are $BO_3$ (peak at 700, 1360 $cm^{-1}$), $BO_4$ (peak at 980 $cm^{-1}$), $SiO_4$ (peak at 470, 1080 $cm^{-1}$), and $PbO_4$ (peak at 470 $cm^{-1}$). Dilatometric measurements indicated that the glass transition temperature and the dilatometric softening point decrease with increasing lead content, whereas the thermal expansion coefficient increases. The change in the dilatometric data with glass composition can be explained on the basis of the change in glass structure with composition, which is confirmed by the results of FTIR spectroscopy. The weaker glass network connectivity and higher polarisability of NBOs formed with increasing PbO content explain the increase in TEC values and the $T_g$ and $T_d$ shift towards lower temperatures. The decrease of volume resistivity with the increasing density and molar volume is associated with the structural changes in the glass network upon increasing PbO content. The change of density and molar volume with PbO content reveals that the increase in density is due to the relatively larger molar mass of lead oxide, while the large ionic radius of the lead ions causes an increase in the molar volume. The volume resistivity decreases with increasing lead content due to the loosening of the glass network. A looser glass network greatly facilitates the movement of $F^-$ ions and $Pb^{2+}$ ions, and hence the conductivity in $PbO–PbF_2–B_2O_3–SiO_2$ glasses increases significantly. The results obtained in this study indicate that the investigated glasses can be potential candidates for advanced technologies as glass-to-metal seals, solder glasses, thick-film pastes, and low-firing glazes.

### Acknowledgements

The authors gratefully acknowledge the financial support from the Ministry of Education and Science of Ukraine (project No. 0118U003396).

## References

[1] S. Arunkumar, K. Venkata Krishnaiah, and K. Marimuthu, Physica B Condens. Matter **416**, 88 (2013); https://doi.org/10.1016/j.physb.2013.02.022
[2] C. A. Gressler and J. E. Shelby, J. Appl. Phys. **64**, 4450 (1988); https://doi.org/10.1063/1.341267
[3] C. A. Gressler and J. E. Shelby, J. Appl. Phys. **66**, 1127 (1989); https://doi.org/10.1063/1.343452
[4] A. G. Souza Filho, J. Mendes Filho, F. E. A. Melo, M. C. C. Custódio, R. Lebullenger, and A. C. Hernandes, J. Phys. Chem. Solids **61**, 1535 (2000); https://doi.org/10.1016/S0022-3697(00)00032-9
[5] A. Wagh, M. I. Sayyed, A. Askin, Ö. F. Özpolat, E. Sakar, G. Lakshminarayana, and S. D. Kamath, Solid State Sci. **96**, 105959 (2019); https://doi.org/10.1016/j.solidstatesciences.2019.105959

[6] D. A. Geodakyan, B. V. Petrosyan, and K. D. Geodakyan, Glass Ceram. **64**, 326 (2007); https://doi.org/10.1007/s10717-007-0083-7
[7] A. Wagh, V. Hegde, C. S. Dwaraka Viswanath, G. Lakshminarayana, Y. Raviprakash, and S. D. Kamath, J. Lumin. **199**, 87 (2018); https://doi.org/10.1016/j.jlumin.2018.03.016
[8] V. I. Goleus, Y. S. Hordieiev, A. V. Nosenko, Voprosy Khimii i Khimicheskoi Tekhnologii **4**, 92 (2018).
[9] A. El-Denglawey, S. A. M. Issa, Y. B. Saddeek, H. O. Tekin, and H. M. H. Zakaly, J. Inorg. Organomet. Polym. Mater. **31**, 3934 (2021); https://doi.org/10.1007/s10904-021-02088-w
[10] B. V. Padlyak, I. I. Kindrat, Y. O. Kulyk, S. I. Mudry, A. Drzewiecki, Y. S. Hordieiev, V. I. Goleus, and R. Lisiecki, Mater. Sci. Eng. B Solid State Mater. Adv. Technol. **278**, 115655 (2022); https://doi.org/10.1016/j.mseb.2022.115655
[11] A. V. Rao, C. Laxmikanth, B. A. Rao, and N. Veeraiah, J. Phys. Chem. Solids **67**, 2263 (2006); https://doi.org/10.1016/j.jpcs.2006.04.012
[12] O. Krupych, I. Martynyuk-Lototska, A. Say, V. Boyko, V. Goleus, Y. Hordieiev, and R. Vlokh, Ukr. J. Phys. Opt. **21**, 47 (2020); https://doi.org/10.3116/16091833/21/1/47/2020
[13] B. G. Rao, H. G. K. Sundar, and K. J. Rao, J. Chem. Soc., Faraday Trans. 1 **80**, 3491 (1984); https://doi.org/10.1039/F19848003491
[14] M. Abid, M. Et-tabirou, and M. Taibi, Mater. Sci. Eng. B Solid State Mater. Adv. Technol. **97**, 20 (2003); https://doi.org/10.1016/S0921-5107(02)00390-2
[15] W. A. Pisarski, J. Pisarska, and W. Ryba-Romanowski, J. Mol. Struct. **744–747**, 515 (2005); https://doi.org/10.1016/j.molstruc.2005.01.022
[16] G. Anjaiah, S. K. Nayab Rasool, and P. Kistaiah, J. Lumin. **159**, 110 (2015); https://doi.org/10.1016/j.jlumin.2014.10.068
[17] W. A. Pisarski, J. Mater. Sci.: Mater. Electron. **17**, 245 (2006); https://doi.org/10.1007/s10854-006-6938-9
[18] J. E. De Souza, J. C. M'Peko, and A. C. Hernandes, Appl. Phys. Lett. **91**, 064105 (2007); https://doi.org/10.1063/1.2767196
[19] J. Pisarska, T. Goryczka, and W. A. Pisarski, Solid State Phenom. **130**, 263 (2007); https://doi.org/10.4028/www.scientific.net/SSP.130.263
[20] I. W. Donald, J. Mater. Sci. **28**, 2841 (1993); https://doi.org/10.1007/BF00354689
[21] J. Coon, M. Horton, and J. E. Shelby, J. Non Cryst. Solids **102**, 143 (1988); https://doi.org/10.1016/0022-3093(88)90125-1
[22] A. Osaka, Y. H. Wang, M. Kobayashi, Y. Miura, and K. Takahashi, J. Non Cryst. Solids **105**, 63 (1988); https://doi.org/10.1016/0022-3093(88)90338-9
[23] M. Wang, L. Fang, M. Li, A. Li, X. Zhang, Y. Hu, Z. Liu, and R. Dongol, Ceram. Int. **45**, 4351 (2019); https://doi.org/10.1016/j.ceramint.2018.11.110
[24] M. Michálková, J. Kraxner, M. Michálek, and D. Galusek, J. Eur. Ceram. Soc. **40**, 2581 (2020); https://doi.org/10.1016/j.jeurceramsoc.2019.11.011
[25] A. E. Ersundu, M. Çelikbilek, and S. Aydin, J. Non Cryst. Solids **358**, 641 (2012); https://doi.org/10.1016/j.jnoncrysol.2011.11.012
[26] J. Massera and L. Hupa, J. Mater. Sci. Mater. Med. 25, 657 (2014); https://doi.org/10.1007/s10856-013-5120-1
[27] S. Baccaro, Monika, G. Sharma, K. S. Thind, D. Singh, and A. Cecillia, Nucl. Instrum. Methods Phys. Res. B **260**, 613 (2007); https://doi.org/10.1016/j.nimb.2007.04.214
[28] B. V. Padlyak, I. I. Kindrat, A. Drzewiecki, V. I. Goleus, and Y. S. Hordieiev, J. Non Cryst. Solids **557**, 120631 (2021); https://doi.org/10.1016/j.jnoncrysol.2020.120631
[29] Y. Cheng, H. Xiao, W. Guo, and W. Guo, Ceram. Int. **33**, 1341 (2007); https://doi.org/10.1016/j.ceramint.2006.04.025
[30] K. S. Shaaban, B. M. Alotaibi, N. Alharbiy, and A. F. A. El-Rehim, Appl. Phys. A **128**, (2022); https://doi.org/10.1007/s00339-022-05474-4
[31] I. Zaitizila, M. K. Halimah, F. D. Muhammad, M. S. Nurisya, M. H. M. Zaid, Chalcogenide Letters **15**, 187 (2018).
[32] V. Kumar, O. P. Pandey, and K. Singh, Physica B: Condensed Matter **405**, 204 (2010); https://doi.org/10.1016/j.physb.2009.08.055

[33] A. Goel, D. U. Tulyaganov, V. V. Kharton, A. A. Yaremchenko, S. Eriksson, and J. M. F. Ferreira, J. Power Sources **189**, 1032 (2009); https://doi.org/10.1016/j.jpowsour.2009.01.013
[24] E. Culea, L. Pop, M. Bosca, T. Rusu, P. Pascuta, and S. Rada, J. Phys. Conf. Ser. **182**, 012061 (2009); https://doi.org/10.1088/1742-6596/182/1/012061
[35] E. Mansour, J. Non Cryst. Solids **358**, 454 (2012); https://doi.org/10.1016/j.jnoncrysol.2011.10.037
[36] Y. B. Saddeek, J. Alloys Compd. **467**, 14 (2009); https://doi.org/10.1016/j.jallcom.2007.11.126
[37] Y. Zhou, Y. Yang, F. Huang, J. Ren, S. Yuan, and G. Chen, J. Non Cryst. Solids **386**, 90 (2014); https://doi.org/10.1016/j.jnoncrysol.2013.11.037